Vascular Pharmacology 122–123 (2019) 106597

Contents lists available at ScienceDirect

Vascular Pharmacology

journal homepage: www.elsevier.com/locate/vph

Negative regulation of eNOS-NO signaling by over-SUMOylation of PPARγ contributes to insulin resistance and dysfunction of vascular endothelium in rats

Wanwan Yuan[a,b,1], Cong Ma[c,1], Yumeng Zhou[a,b], Mengxi Wang[a,b], Guohua Zeng[a,b], Qiren Huang[a,b,*]

[a] Key Provincial Laboratory of Basic Pharmacology, Nanchang University, Nanchang, Jiangxi 330006, PR China
[b] Department of Pharmacology, School of Pharmacy, Nanchang University, Nanchang, Jiangxi 330006, PR China
[c] Jiangxi Medical College, Nanchang University, Nanchang, Jiangxi 330006, PR China

ARTICLE INFO

Keywords:
Insulin resistance
SUMOylation
Peroxisome proliferator-activated receptor gamma
Endothelium
Angiopathy

ABSTRACT

SUMOylation of peroxisome proliferator-activated receptor gamma (PPAR γ) plays important regulatory role in its transcriptional activity. Our recent studies in vitro found that over-SUMOylation of PPARγ, like high glucose and high fat (HG/HF), induced endothelial insulin resistance (IR). However, whether such an event occurs in rats remains unclear. Therefore, our study aimed at investigating whether PPARγ over-SUMOylation could mimic high sucrose/fat diet (HFD) to induce endothelial IR and dysfunction and explored its underlying mechanisms. Normal chow-fed rats were intravenously infected with adenoviruses carrying the wild type cDNAs encoding PPARγ, SUMO1 and PIAS1 (protein inhibitor of activated STAT1). HFD-fed rats were regarded as a positive control. Body physical and biochemical parameters, glucose tolerance and vessel function were detected. The expression and SUMOylation levels of PPARγ were measured by western blotting and co-immunoprecipitation. Our results showed that like HFD, PPARγ over-SUMOylation induced endothelial IR and dysfunction via a negative regulation of eNOS-NO pathway. More importantly, we found that PPARγ over-SUMOylation induced endogenous SUMOylation cascade and exacerbated endothelial IR and dysfunction.The findings will deepen the understanding on PPARγ SUMOylation-regulating insulin signaling network and offer a potential target for prevention and cure of diabetic vascular complications.

1. Introduction

Peroxisome proliferator-activated receptor gammar (PPARγ) is a target of thiazolidinediones (TZDs) which are used to treat the patients with type 2 diabetes mellitus (T2DM). It plays important roles in enhancement of insulin sensitivity, pro-adipogenesis and anti-inflammation through PPARγ response element (PPRE) dependent trans-activation and/or PPRE independent trans-repression [1–3]. Numerous studies have demonstrated that post-translational modifications of PPARγ regulate its transcriptional activity [4–6]. Of these modifications, PPARγ SUMOylation is the most important negative regulatory manner [7]. It is reported that the PPARγ SUMOylation commonly occurs in macrophages, adipose tissues and skeletal muscles and so forth [8,9]. However, it is not fully clear whether it occurs in vessel tissues. Recently, we found that the SUMOylation of PPARγ and endothelial insulin resistance (IR) also took place in the cultured vascular endothelial cells induced by the stress of high glucose and high fat (HG/HF) [10]. Thus, an interesting question is raised whether the SUMOylation of PPARγ could mimic the high sucrose/fat diet (HFD) to induce endothelial IR and dysfunction in rats.

Endothelial IR is known as a decrease of response of vascular endothelial cells to insulin, presenting a decrease in endothelium-derived nitric oxide (NO) and/or an increase in angiotensin II (AngII) induced by insulin and it precedes endothelial dysfunction [11]. Moreover, it is a trigger of diabetic vascular complication such as hypertension, atherosclerosis [12,13]. It is believed that hyperglycemia induces the

Abbreviations: AngII, angiotensin II; eNOS, endothelial nitric oxide synthase; ET-1, endothelin-1; HFD, high sucrose/fat diet; IκBα, inhibitory κB alpha; IKK, inhibitory κB kinase; iNOS, inducible nitric oxide synthase; IR, insulin resistance; NFκB, nuclear factor κB; NO, nitric oxide; PIAS1, protein inhibitor of activated STAT1; PPARγ, peroxisome proliferator-activated receptor gamma; ROS, reactive oxygen species; T2DM, type 2 diabetes mellitus; TZDs, thiazolidinediones

* Corresponding author at: Key Provincial Laboratory of Basic Pharmacology, Nanchang University, 461 Ba-Yi Street, Nanchang, Jiangxi 330006, PR China.
E-mail address: qrhuang@ncu.edu.cn (Q. Huang).

[1] Equal contribution to this article.

https://doi.org/10.1016/j.vph.2019.106597
Received 17 April 2019; Received in revised form 22 August 2019; Accepted 30 August 2019
Available online 31 August 2019
1537-1891/

production of reactive oxygen species (ROS) and ROS activates inhibitory κB kinase (IKK). Activated IKK interacts with insulin receptor substrate 1(IRS1) and phosphorylates it at serine 312, which impedes the binding of IRS1 to PI3K and inhibits downstream eNOS-NO pathway, thus resulting in the endothelial IR and dysfunction [14]. However, it remains unclear whether the PPARγ SUMOylation could mimic the HFD to inhibit the eNOS-NO pathway. Accordingly, in the present study, we focuses on investigating whether over-SUMOylation of PPARγ could simulate HFD to induce the endothelial IR and dysfunction in rats and explored its likely mechanisms.

2. Materials and methods

2.1. Materials

Adenoviruses including Ad-HA-PPARγ, Ad-Myc-SUMO1 and Ad-Flag-PIAS1 were prepared and purchased from Genechem Co. (Shanghai, CHN). Antibodies against PPARγ, SUMO1 and PIAS1 were purchased from Abcam (NY, USA). Other antibodies against PI3K, AKT, eNOS, IKK, IKK-pS176 and β-actin were purchased from Cell Signaling Technologies (MA, USA). The kits for fasting plasma glucose (FPG), triglyceride (TG), total cholesterol (TCH), malonaldehyde (MDA), superoxide dismutase manganese (SOD−Mn), glutathione peroxidase (GSH-Px) and NO were purchased from Nanjing Jiancheng Bioengineering Institute (Nanjing, CHN). Serum insulin and Ang II assay kits were from CUSABIO (Wuhan, CHN). Other chemicals used here were purchased from Solarbio Co. (Beijing, CHN).

2.2. Establishment of systemic and endothelial IR model and adenovirus infection in rats

All animal procedures were approved by the Institutional Animal Care and Use Committee of Nanchang University School of Medicine and conducted in accordance with the guide for the Care and Use of Laboratory Animals published by the US National Institute of Health (NIH Publication No.85-23, revised 1996). Twenty-four male Sprague Dawley (SD) rats were purchased from Nanchang University School of Medicine. The rats were fed with a normal chow and acclimated at a SPF environment where the temperature was approximately 25 °C and the humidity was about 50% for a week. Twenty-four male rats were randomized into the HFD group (6 rats, as a positive control) fed with a high sugar and fat diet for 16 weeks (D12492, Open Source Diets™, USA) and the normal group (18 rats) fed with a normal chow for 16 weeks. After 16 weeks of feeding, 18 normal rats were randomly allocated into normal control (Ctrl), negative control (Vehicle) and adenovirus-co-infection group (Ad). The rats in Ad group were intravenously infected with the viruses containing Ad-HA-PPARγ, Ad-Myc-SUMO1 and Ad-Flag-PIAS1 at a ratio of 1:1:1; whereas the rats in Vehicle group were intravenously infected with adenoviruses without containing these vectors. After infection with adenovirus, all the animals were kept feeding as above-mentioned for an additional 4 weeks.

2.3. Measurement of physical and biochemical parameters

After 4 weeks of adenovirus injection, the rats were fasted for 12 h. Before detecting the physical and biochemical parameters, the rats were first anesthetized with isoflurane. Body length (from nose-tip to anus) and body weight were then measured. Blood samples were collected from retro-orbital plexus using capillary tubes and serum was prepared. Serum biochemical parameters were determined following the instructions of manufacturers' kits commercially available. Serum insulin and AngII levels were measured by enzyme-linked immunosorbent assay (ELISA).

2.4. Oral glucose tolerance test (OGTT)

The rats were fasted overnight and the fasting plasma glucose levels were measured. Then the rats were orally administered with glucose solution (2 g/kg). At 15 min, 30 min, 60 min, 120 min and 180 min after glucose loading, blood samples were collected and the plasma glucose levels were measured.

2.5. Detection of endothelium-dependent vasodilation function in vivo

The detection of endothelium-dependent vasodilation function in vivo was performed according to the methods described in papers with minor modifications [15–17]. Acetylcholine (Ach) and sodium nitroprusside (SNP) were respectively dissolved in 9% NaCl and prepared to desired concentrations. After anesthetized with isoflurane, the rats were subcutaneously (sc) injected with insulin (5 IU/kg), and intraperitoneally (ip) injected with Ach (0.05 g/kg and 0.5 g/kg) and SNP (0.05 g/kg and 0.5 g/kg), respectively. After each administration, inner wall of left carotid artery was visualized and inner diameter of the artery was recorded by an Ultra-high Resolution Small Animal Ultrosound Imaging Instrument (Vevo 2100, Toronto, CAN).

2.6. Detection of endothelium-dependent vasodilation function in vitro

Rats were anesthetized with isoflurane and sacrificed by cervical dislocation. Thoracic aorta in whole was rapidly taken out and placed in a pre-cooled oxygen-enriched Kreb-Henseleit (K−H) solution (82.8 $mmol.L^{-1}$ NaCl, 4.7 $mmol.L^{-1}$ KCl, 2.4 $mmol.L^{-1}$ KH_2PO_4, 1.2 $mmol.L^{-1}$ $MgSO_4$, 2.7 $mmol.L^{-1}$ $CaCl_2$, 11.1 $mmol.L^{-1}$ dextrose, and 25 $mmol.L^{-1}$ $NaHCO_3$, *p*H 7.4, 37 °C). After removal of the adipose tissue peri-vascular, the aorta was cut into approximately 2–3 mm rings. One of the vessel rings was used to detect the endothelium-dependent vasodilation function and others were quickly frozen and used to detect protein expression levels and SUMOylation levels by western blots and co-immunoprecipitation. The aortic ring was isometrically mounted in 10 mL organ baths filled with pre-warmed K−H solution (37.0 °C) continuously gassed with 95%O_2–5%CO_2 in a myograph system (model 620 M, DMT, Denmark). An initial passive tension in aortic ring was set at 2.0 g. The aortic ring was first allowed to equilibrate in K−H solution for at least 60 min and then its contraction response was detected by addition of 10^{-9}–10^{-5} $mol.L^{-1}$ phenylephrine (PE). After detection of contraction response, the aortic ring was equilibrated for 60 min and pre-contracted again with 10^{-6} $mol.L^{-1}$ PE. Subsequently, a dose-response curve was prepared by cumulative addition of Ach (10^{-9}–10^{-3} $mol.L^{-1}$) and SNP (10^{-9}–10^{-3} $mol.L^{-1}$), respectively. Finally, vasodilation function was calculated as follows: endothelium-dependent vasodilation function = [(pre-contraction plateau value-tension value at a concentration) / (pre-contraction plateau value-2.0 g)] × 100%.

2.7. Western blotting analysis

Frozen aorta tissues were homogenized and lysed with lysis buffer (50 mM Tris-HCl (pH 7.4), 150 mM NaCl, 1% NP-40, 0.1% SDS) on ice for 10 min. Then the lysates were clarified by centrifugation at 12,000 × *g* for 15 min. Protein concentration was measured with BCA protein quantification kit (Applygen, Beijing, CHN). Equal amount of lysates was separated by SDS-PAGE and transferred to polyvinyl difluoride membrane. The membrane was subsequently blocked with milk and incubated with specific primary antibodies at a 1:1000 dilution, followed by incubating with a horseradish peroxidase conjugated secondary antibody at a 1:5000 dilution, and finally detected with chemiluminescence (ECL, Tiangen, CHN).

2.8. Co-immunoprecipitation assay

Frozen aorta tissues were homogenized with lysis buffer (50 mM Tris-HCl (pH 7.4), 150 mM NaCl, 1% NP-40, 0.1% SDS) on ice for 10 min. The lysates were then clarified by centrifugation at 12,000 ×*g* for 15 min. Protein concentration was measured with BCA protein quantification kit (Applygen, Beijing, CHN). Equal amount of lysates was incubated with the antibody against PPARγ overnight at 4C. Protein A + G-Sepharose (Sigma) was added and incubated for 3 h at 4 °C. After three gentle washes with immuno-precipitation buffer, the immuno-precipitates were detected by western blotting assay.

2.9. Statistical analysis

Statistical analysis was performed using Graphpad prism version 7.0. All experimental data were expressed as mean ± S.D. Homogeneity of variance and one-way ANOVA were used where applicable. Inter-group comparisons were performed using the Student's *t*-test. *P* value less than 0.05 was considered significant difference.

3. Results

3.1. Identification of over-SUMOylation of PPARγ in rat aorta

Western blotting results showed that expressions of PPARγ, SUMO1 and PIAS1 in Ad group were significantly higher than those in Ctrl or Vehicle group, suggesting that the virus co-infection was successful (Fig. 1a–d). While the expression of PIAS1 in HFD group was higher than that in Ctrl or Vehicle group, there was no significant difference between HFD and Ad group (Fig. 1d), indicating HFD, like the virus co-infection, induced the SUOMylation of PPARγ, which was supported from the co-immunoprecipitation results. As shown in Fig. 1e and f, the co-immuno-precipitation results displayed that the SUMOylation levels of PPARγ in both HFD and Ad group were strikingly higher than those in Ctrl or Vehicle group, suggesting that the co-infection of the viruses has a similar effect as HFD to induce PPARγ SUOMylation in rat aorta tissue.

3.2. Over-SUMOylation of PPARγ induces systemic IR in rats

Next, we observed the effects of over-SUMOylation of PPARγ on systemic IR by detecting the body physical parameters and serum biochemical parameters. While no notable change in body length was observed, HFD caused marked increases in body weight, TG, TCH, FPG, INS and HOMA-IR index, demonstrating that HFD induced the systemic IR in rats. Similarly, the co-infection of these viruses (Ad group) also resulted in noticeable elevations in the parameters mentioned above, indicating that over-SUMOylation of PPARγ simulated HFD to induce the systemic IR in rats (Fig. 2a–g).

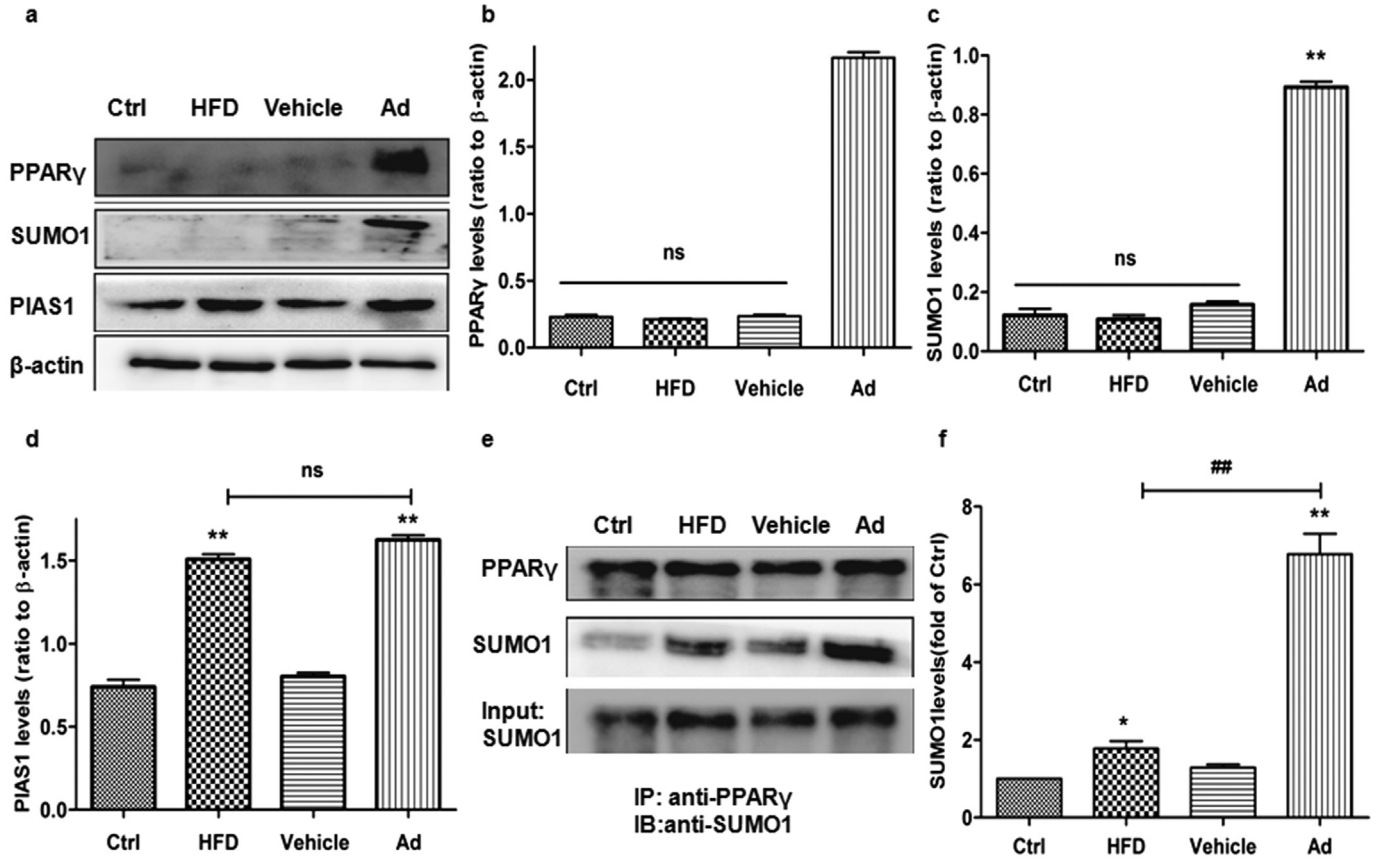

Fig. 1. Identification of over-SUMOylation of PPARγ in rat aorta.
Twenty-four male rats were randomized into HFD group (6 rats) fed with HFD and normal group (18 rats) fed with a normal chow for 16 weeks. After 16 weeks of feeding, the normal rats were randomly sub-grouped into control (Ctrl), negative control (Vehicle) and adenovirus co-infection (Ad) group. The rats in Ad group were intravenously co-infected with the viruses containing Ad-HA-PPARγ, Ad-Myc-SUMO1 and Ad-Flag-PIAS1; whereas the rats in Vehicle group were intravenously infected with adenoviruses without carrying these vectors. After infection, all of the animals were kept feeding with corresponding diets for an additional 4 weeks. Finally, the rats were anesthetized with isoflurane and sacrificed by cervical dislocation. Expression of PPARγ (a, b), SUMO1 (a, c), PIAS1 (a, d) and the PPARγ SUMOylation levels (e, f) were detected by western blotting and co-immunoprecipitation in rat aortic tissues. All data were expressed as mean ± S.D. of 6 rats. One-way ANOVA and the Student's *t*-test were performed. *$P < 0.05$, **$P < 0.01$, vs. Ctrl or Vehicle; ## $P < 0.01$, vs. HFD; ns: no significance.

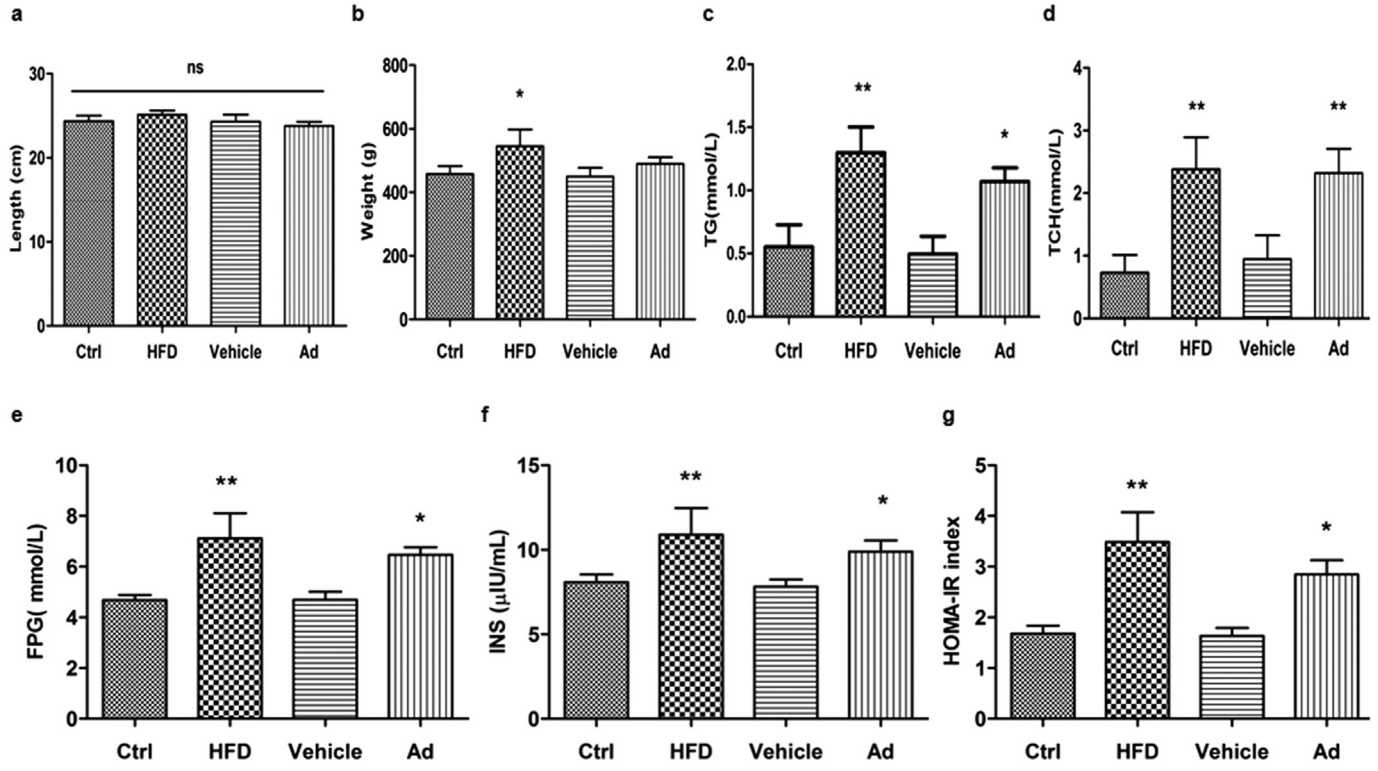

Fig. 2. Over-SUMOylation of PPARγ induces systemic IR in rats.
Grouping was described as the legend of Fig. 1. The rats in Ad group were intravenously co-infected with the viruses containing Ad-HA-PPARγ, Ad-Myc- SUMO1 and Ad-Flag-PIAS1; whereas the rats in Vehicle group were intravenously infected with adenoviruses without carrying these vectors. After infection, all of the animals were kept feeding with corresponding diets for an additional 4 weeks. Finally, the rats were fasted overnight and anesthetized with isoflurane. Body length (a) and weight (b) were measured. Serum triglyceride (TG, c), total cholesterol (TCH, d), fasting plasma glucose (FPG, e), insulin (INS, f) and HOMA-IR index (g) were detected. All data were expressed as mean ± S.D. of 6 rats. One-way ANOVA and the Student's *t*-test were performed. $*P < 0.05$, $**P < 0.01$, vs. Ctrl or Vehicle; ns: no significance.

3.3. Over-SUMOylation of PPARγ results in systemic glucose intolerance and endothelial IR in rats

The OGTT results showed that exposure of rats to HFD exhibited a notable glucose intolerance compared with Ctrl group or Vehicle group. Co-infection of these viruses (Ad) executed a similar effect as HFD, indicating that over-SUMOylation of PPARγ, like HFD, impaired the systemic glucose tolerance(Fig. 3a and b). Subsequently, we evaluated the effects of over-SUMOylation of PPARγ on the endothelial IR by detecting the serum levels of NO and Ang II and measuring the vasodilation function in response to insulin challenge. The levels of NO and Ang II in both HFD and Ad group were significantly higher than those in Ctrl or Vehicle group (Fig. 3c and d), which was inconsistent with our previous results in vitro. We assumed that the increase of NO levels in HFD and Ad group might be due to the activation of inducible NOS (iNOS). To test the possibility, aminoguanidine (AG), a selective iNOS inhibitor, was used. As expected, treatment with AG (100 mg/kg) abrogated the increase of NO levels induced by HFD or Ad, indicating that the increases of NO levels induced by over-SUMOylation of PPARγ are mainly dependent on iNOS activation (Supplementary Fig. 1). What is more, in response to insulin, the inner diameter of carotid artery in both HFD and Ad group were markedly lower than those in Ctrl or Vehicle group, indicating over-SUMOylation of PPARγ, like HFD, results in the endothelial IR (Fig. 3e).

3.4. Over-SUMOylation of PPARγ impairs endothelium-dependent vasodilation function in vitro

To directly attest whether the endothelial IR occurred in Ad group, an assay of endothelium-dependent vasodilation function in vitro is required. The results showed that Ach-induced endothelium-dependent vasodilation response, either in HFD or Ad group, was markedly lower than that in Ctrl or Vehicle group; moreover, the response was presented in a concentration-dependent manner (Fig. 4a and b). However, compared with Ctrl or Vehicle group, no notable alteration of endothelium- independent vasodilation response induced by SNP was found in either HFD or Ad group (Fig. 4c and d). These data demonstrate that over-SUMOylation of PPARγ results in the endothelium-dependent vasodilation dysfunction.

3.5. Effects of over-SUMOylation of PPARγ on vascular diastolic function in vivo

We subsequently investigated the effects of over-SUMOylation of PPARγ on vascular diastolic function in vivo by an ultra-sound imaging technique. The results revealed that the left carotid arteries from both control rats (Ctrl) and vehicle rats (Vehicle) manifested a nearly linear dose-dependent vasodilation response to Ach. However, the arteries from rats treated with either HFD or co-infection (Ad) failed to display the dose-dependent vasodilation response to Ach and the vasodilation responses were weaker than those in Ctrl or Vehicle group (Fig. 5a and b). In contrast, while endothelium-independent vasodilation responses to SNP in all groups presented a linear dose-dependent vasodilation response to a certain extent, there were no significant differences between these groups (Fig. 5c and d). The finding further indicates that over-SUMOylation of PPARγ causes the endothelial IR and impaired endothelium-dependent vasodialtion function.

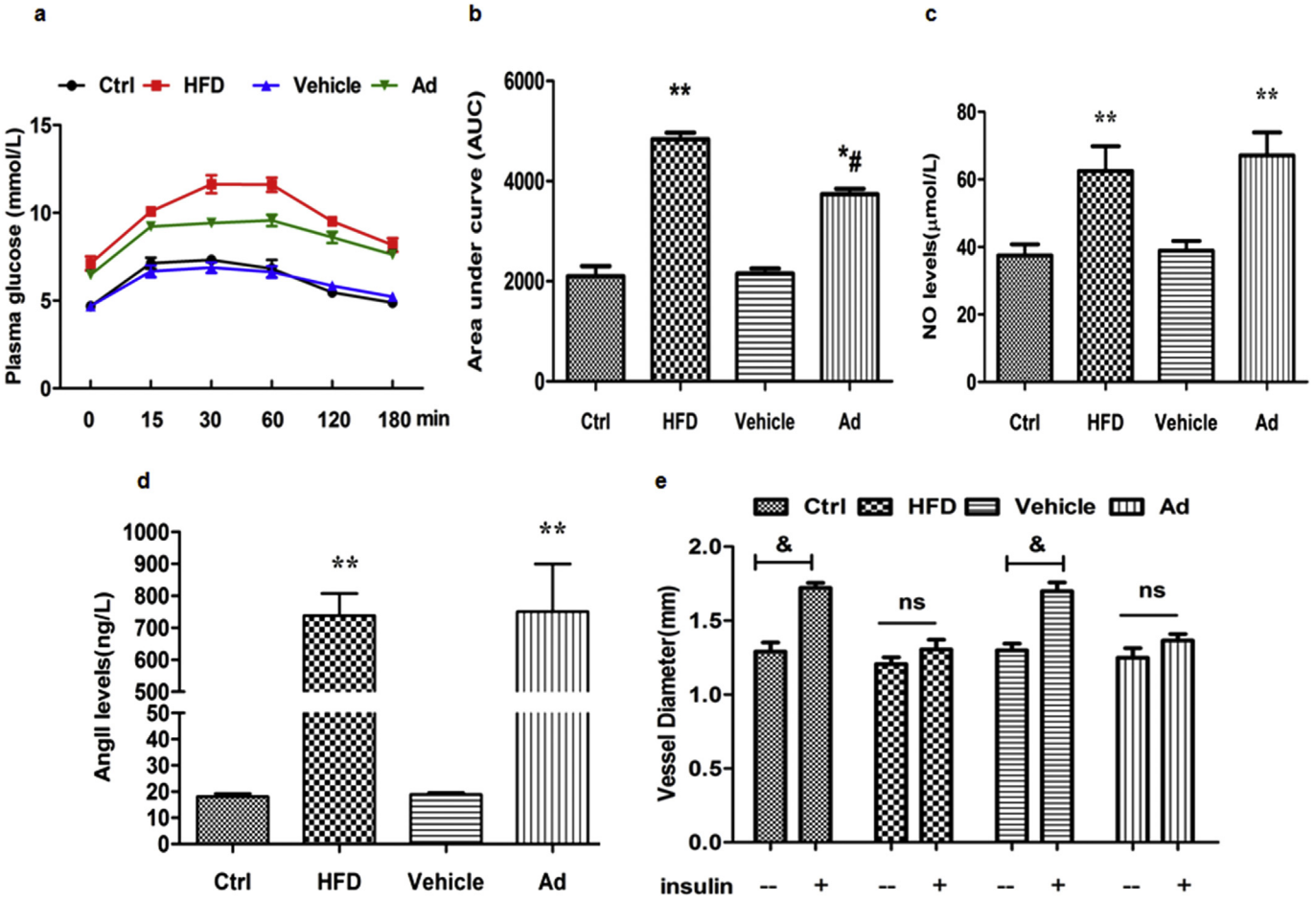

Fig. 3. Over-SUMOylation of PPARγ results in systemic glucose intolerance and endothelial IR in rats.
Grouping and processing were described as the legend of Fig. 2. The rats were fasted overnight and the fasting plasma glucose levels were measured. Then the rats were orally administered with glucose solution (2 g/kg). At 15 min, 30 min, 60 min, 120 min and 180 min after glucose loading, blood samples were drawn and the plasma glucose levels were measured. The curve of the plasma glucose levels varied with time (a) was prepared and the area under curve (AUC) in each group was calculated (b). In addition, the levels of NO (c) and Ang II (d) were detected, respectively.The inner diameter of carotid artery stimulated with or without insulin (5 IU/kg, sc) was measured with an ultro-sound imaging instrument (e). All data were expressed as mean ± S.D. of 6 rats. One-way ANOVA and the Student's *t*-test were performed. $^{*}P < 0.05$, $^{**}P < 0.01$, vs. Ctrl or Vehicle; $\#P < 0.05$, vs. HFD group; & $P < 0.05$, ns: no difference, vs. without insulin.

3.6. Over-SUMOylation of PPARγ contributes to vascular oxidative stress

Subsequently, we sought to explore how over-SUMOylation of PPARγ causes the endothelial IR and impaired endothelium-dependent vasodialtion function. The results showed that HFD significantly elevated the contents of MDA whereas lowered the activities of SOD-Mn and GSH-Px in vascular tissues. Moreover, over-SUMOylation of PPARγ had a similar effect as HFD (Fig. 6a–c), suggesting that like HFD, over-SUMOylation of PPARγ also results in vascular oxidative stress.

3.7. Over-SUMOylation of PPARγ activates IKK and promotes interaction between IKK and PIAS1 in rat aorta

The results of western blotting showed that the expression of IKK-pS176 in either HFD group or Ad group was significantly higher than that in Ctrl or Vehicle group, demonstrating that over-SUMOylation of PPARγ can activate IKK, an upstream kinase of inflammation pathway (Fig. 7a). Moreover, co-immunoprecipitation further displayed an obvious interaction between IKK and PIAS1 in either HFD group or Ad group, compared with Ctrl or Vehicle group (Fig. 7b), indicating that over-SUMOylation of PPARγ promotes the interaction between IKK and PIAS1.

3.8. Over-SUMOylation of PPARγ down-regulates PI3K-AKT-eNOS pathway in rat aorta

Finally, we investigated the effects of over-SUMOylation of PPARγ on endothelial insulin pathway. Compared with Ctrl group, the expressions of PI3K, AKT and eNOS in HFD group were significantly decreased; likewise, the PI3K, AKT and eNOS expression levels in Ad group were significantly lower than those in Vehicle group, suggesting that over-SUMOylation of PPARγ down-regulates PI3K-AKT-eNOS pathway in rat aorta (Fig. 8a–d).

4. Discussion

IR is associated closely with metabolic disorders (dyslipidemia, glucose intolerance and visceral obesity) and cardiovascular diseases (hypertension and atherosclerosis) and it is a marker of metabolic syndrome [18–20]. Although the pathogenesis of T2DM is not fully elucidated, it has been confirmed that IR plays a key role in the onset and development of T2DM [21]. It is well known that long-term HFD leads to IR in humans and animals [22,23]. However, the molecular mechanism underlying IR has not yet been completely characterized. In the past two decades, vascular endothelial cells and vascular smooth muscle cells were commonly considered as insulin-sensitive cells [24]. Insulin plays important roles in cardiovascular system including

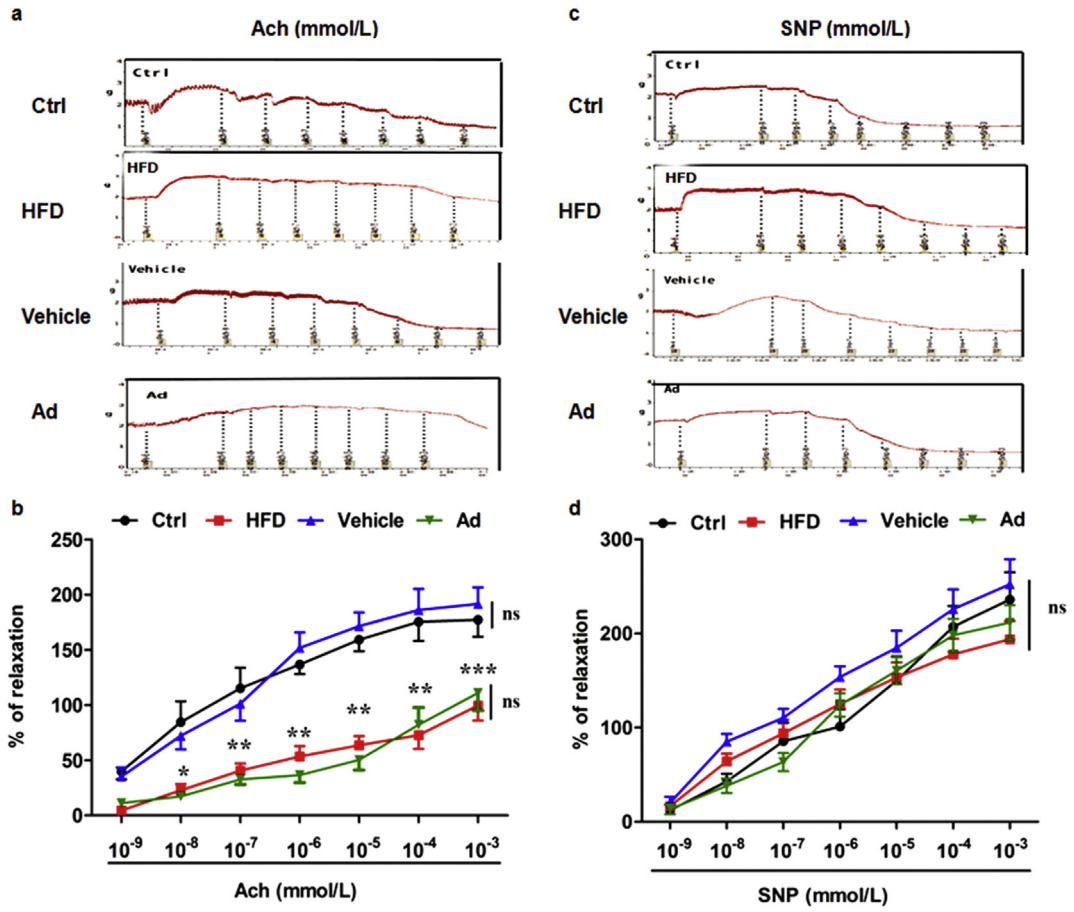

Fig. 4. Over-SUMOylation of PPARγ impairs endothelium-dependent vasodilation function in vitro.
Grouping and processing were described as the legend of Fig. 2. The rats were anesthetized with isoflurane and sacrificed by cervical dislocation. Thoracic aorta was quickly taken out and cut into approximately 2-3 mm rings. The aortic rings were isometrically mounted in 10 mL organ baths filled with pre-warmed K—H solution continuously gassed with 95%O_2–5%CO_2 in a myograph system. The aortic rings were pre-contracted with 10^{-6} mol.L^{-1} phenylephrine (PE). Dose-response curve was obtained by cumulative addition of acetylcholine (Ach, 10^{-9}–10^{-3} mol.L^{-1}, a, b) and sodium nitroprusside (SNP, 10^{-9}–10^{-3} mol.L^{-1}, c, d). All data were expressed as mean ± S.D. of 6 rats. One-way ANOVA and the Student's *t*-test were performed. *$P < 0.05$, **$P < 0.01$, ***$P < 0.001$, vs. Ctrl or Vehicle; ns: no significance.

maintenance of vascular endothelium integrity and regulation of vascular tension [25,26]. These roles are achieved through a balance between NO and AngII/ET1. Accordingly, the levels of NO and AngII/ET1 are commonly regarded as indicators of endothelial function [27]. However, numerous risk factors including hyperglycemia, hyperlipidemia, hyperhomocysteinemia and so forth impair endothelial function and result in endothelial dysfunction and IR through various mechanisms including oxidative stress, inflammation, and apoptosis [28–30]. It has been documented that PPARγ plays critical roles in modulating homeostasis of glucose and lipid, insulin sensitivity, adipogenesis and inflammation. Its synthesized ligands such as TZDs are applied to clinical practice [31–33]. Growing basic and clinical evidence has shown that TZDs ameliorate IR state of the patients with T2DM and they are beneficial for prevention and treatment of diabetic angiopathy [34].

While PPARγ exerts a positive effect on systemic insulin sensitivity, recent researches have proposed that SUMOylation of PPARγ may execute a negative effect on systemic insulin sensitivity [35]. In adipose tissue, SUMOylation of PPARγ2 at Lys107 negatively regulates the transcriptional activity of PPARγ2 because the mutation of 107 K to R showed increased transcriptional activity [36]. In macrophages, the SUMOylation of PPARγ1 at Lys365 negatively regulates the expression of inflammatory genes such as iNOS and TNF-α, which are regulated by NF kappa B [37]. In our cell-based in vitro studies, we recently found that SUMOylation of PPARγ can simulate HG/HF stress to induce the endothelial IR (data not shown). However, whether this effect occurs in vivo remains unclear. In this study, our aim was to explore whether over-SUMOylation of PPARγ could mimic the endothelial IR and dysfunction induced by HFD in rats. Rats were co-infected with the viruses carrying wild type cDNAs encoding PPARγ, SUMO1 and PIAS1. Our results showed the expression levels of PPARγ, SUMO1 and PIAS1 and the SUMOylation levels of PPARγ in rat aorta indeed significantly increased in Ad group, indicating that the co-infection of viruses was successful.

Patients with IR syndrome commonly manifest over-weight, hyperglycemia, dyslipidemia, hyperinsulinemia, etc. [38]. Indeed, our present results displayed over-SUMOylation of PPARγ, like HFD, also brought about phenotype changes in rats. Moreover, impaired glucose tolerance was observed. Consequently, the rats in Ad group manifested the phenotype of systemic IR. Then, we next wondered whether the rats in Ad group manifested the endothelial IR. As expected, over-SUMOylation of PPARγ, like HFD, also significantly elevated the levels of AngII and NO. The result appears to be conflict with the notion of endothelial IR. In fact, it is not conflict at all, because what we detected is serum total NO levels which derive from both eNOS in endothelium and iNOS in other tissues [39]. Moreover, the results from both ours and others demonstrate that the serum NO levels come primarily from iNOS in inflammatory state (Supplementary Fig. 1) [40]. Therefore, it is not enough to really reflect endothelial function only by detecting the serum NO levels. It is necessary to directly evaluate the endothelial

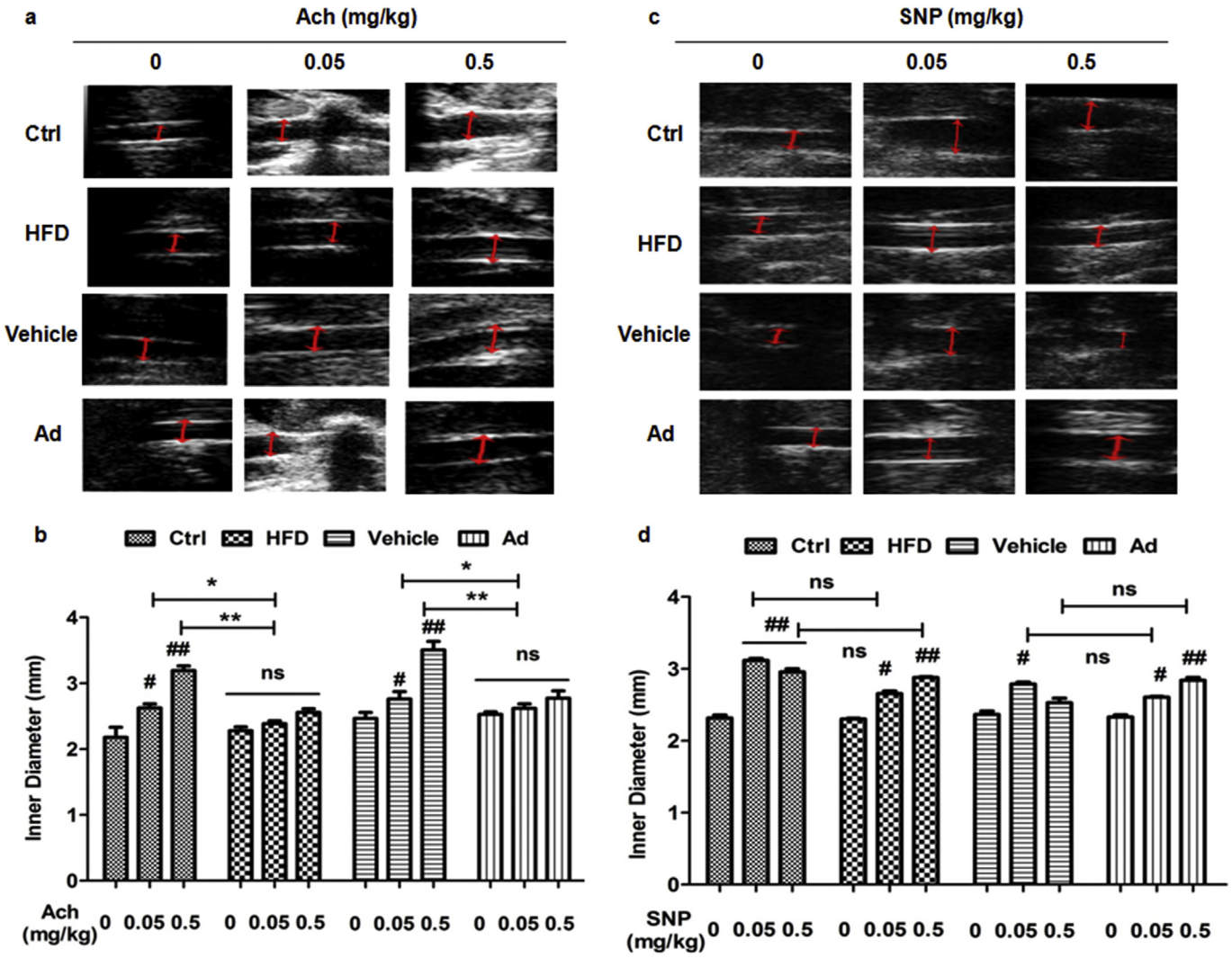

Fig. 5. Effects of over-SUMOylation of PPARγ on vascular diastolic function in vivo.
Grouping and processing were described as the legend of Fig. 2. After anesthetized with isoflurane,and the rats were intra-peritoneally injected with Ach at doses of 0.05 g/kg and 0.5 g/kg (a, b) and SNP at doses of 0.05 g/kg, 0.5 g/kg (c, d), respectively. After each administration, the inner diameter of left carotid artery was visualized and analyzed by an an ultro-sound imaging instrument. All data were expressed as mean ± S.D. of 6 rats. One-way ANOVA and the Student's *t*-test were performed. $*P < 0.05$, $**P < 0.01$, vs. Ctrl or Vehicle; $\#P < 0.05$, $\#\#P < 0.01$, vs. 0 g/kg; ns: no significance.

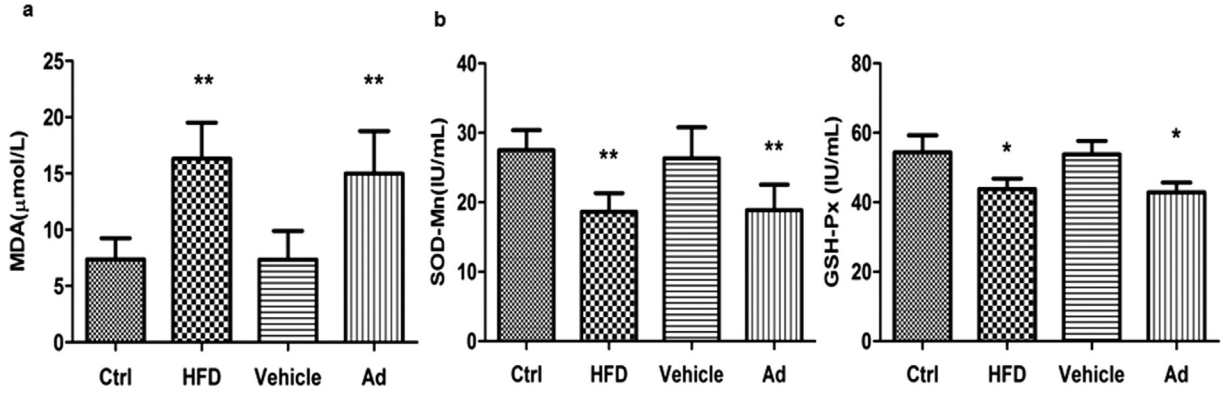

Fig. 6. Over-SUMOylation of PPARγ contributes to vascular oxidative stress.
Grouping and processing were described as the legend of Fig. 2. At the end, the rats were anesthetized with isoflurane and sacrificed by cervical dislocation. Thoracic aorta was quickly taken out and homogenate was prepared. MDA contents (a) and the activities of SOD-Mn (b) and GSH-Px (c) were detected in rat aorta tissues. All data were expressed as mean ± S.D. of 6 rats. One-way ANOVA and the Student's *t*-test were performed. $*P < 0.05$, $**P < 0.01$, vs. Ctrl or Vehicle.

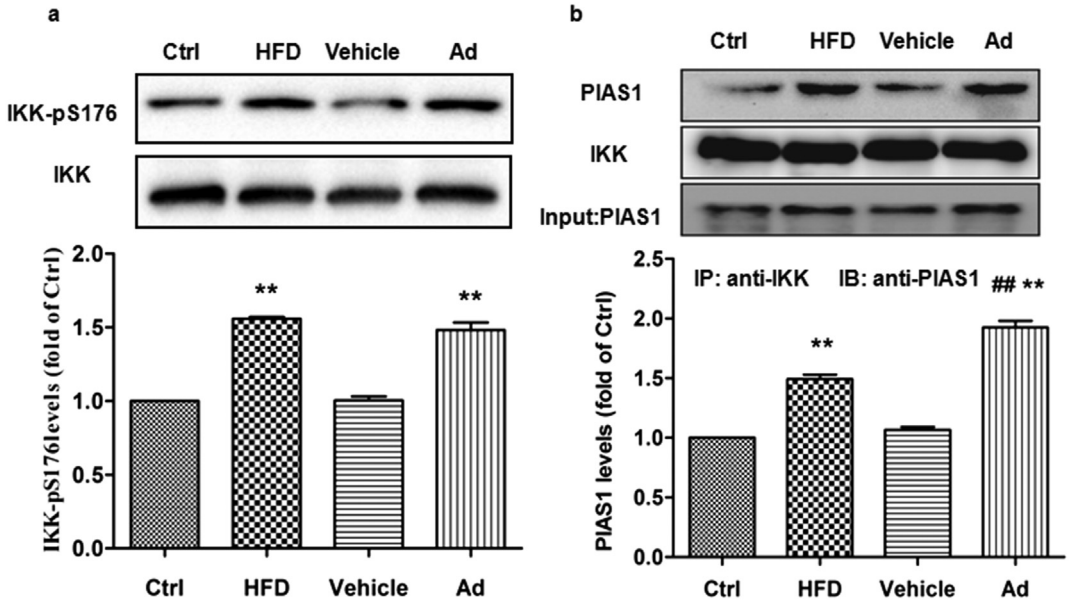

Fig. 7. Over-SUMOylation of PPARγ activates IKK and promotes interaction between IKK and PIAS1 in rat aorta.
Grouping and processing were described as the legend of Fig. 2. At the end, the rats were anesthetized with isoflurane and sacrificed by cervical dislocation. Aorta tissues were used for detecting the levels of IKK and IKK-pS176 (a) by western blotting and the interaction between IKK and PIAS1 by co-immunoprecipitation (b). All data were expressed as mean ± S.D. of 6 rats. One-way ANOVA and the Student's *t*-test were performed. $^{**}P < 0.01$, vs. Ctrl or vehicle; $\#\#P < 0.01$, vs. HFD group.

function both in vitro and in vivo in response to insulin, Ach and SNP. The vascular dilation function includes endothelium-dependent induced by Ach and endothelium-independent dilation function triggered by NO donor such as SNP. Only the endothelium-dependent dilation function induced by Ach really reflects the endothelium function [41].

It is well known that Ach induces the expression and/or activation of eNOS which converts L-arginine to NO in endothelial cells. Subsequently, NO diffuses into vascular smooth muscle cells where it binds to a soluble guanylate cyclase (sGC) which converts GTP to cGMP. Cyclic GMP is a second messenger which mediates the vessel dilation [42].

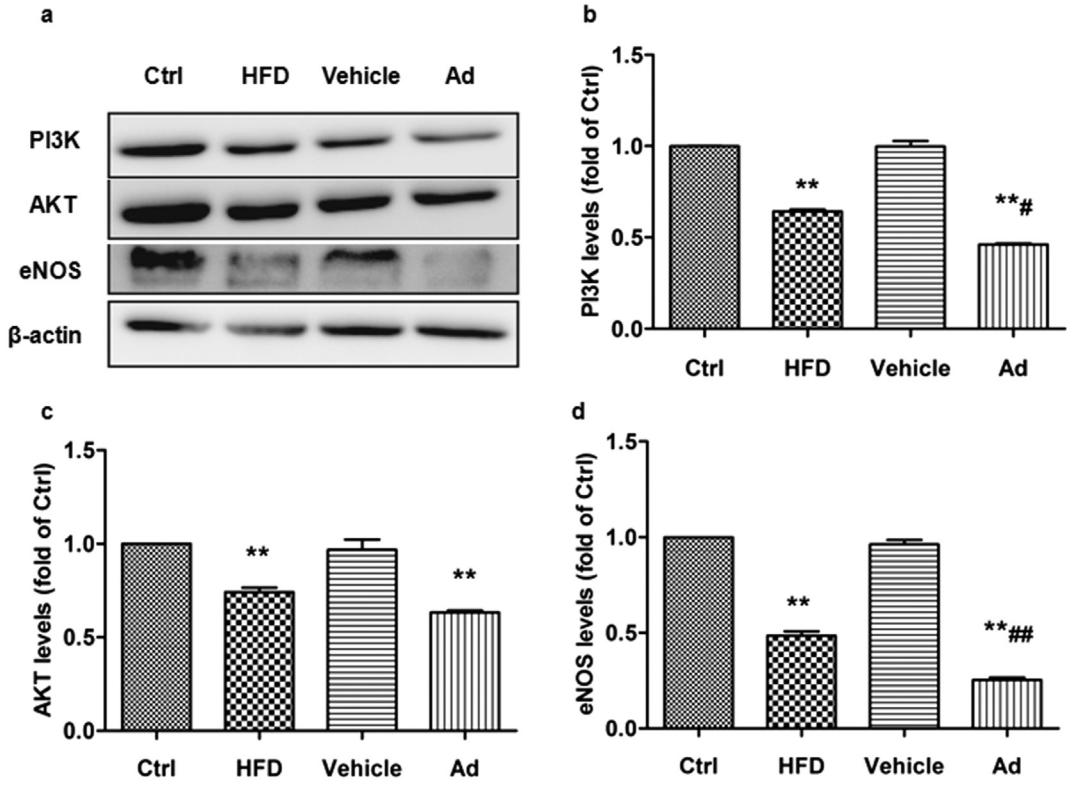

Fig. 8. Over-SUMOylation of PPARγ down-regulates PI3K-AKT-eNOS pathway in rat aorta.
Grouping and processing were described as the legend of Fig. 2. At the end, the rats were anesthetized with isoflurane and sacrificed by cervical dislocation. Aorta tissues were used for detecting the levels of PI3K (a, b), AKT (a, c) and eNOS (a, d) by western blotting, β-actin as a loading control. All data were expressed as mean ± S.D. of 6 rats. One-way ANOVA and the Student's *t*-test were performed. $^{**}P < 0.01$, vs. Ctrl or Vehicle; $\#P < 0.05$, $\#\#P < 0.01$, vs. HFD group.

Our present results displayed over-SUMOylation of PPARγ impaired the endothelium-dependent instead of the endothelium-independent vasodilation function both in vitro and in vivo.

Numerous lines of evidence have indicated that oxidative stress induced by hyperglycemia is an important mechanism underlying the endothelial IR [43]. The next issue we concerned was whether over-SUMOylation of PPARγ could affect the vascular oxidative stress incurred by ROS. It is well believed that dynamics of ROS is very important for maintaining organism homeostasis. Maintenance of ROS homeostasis relies on the balance between production and clearance of ROS. ROS are primarily produced by oxidative phosphorylation of glucose in mitochondria and cleared by anti-oxidative system including GSH-Px, SOD-Mn and catalase etc. [44]. Once the balance is disturbed, a great amount of ROS would accumulate and then cell injury would occur [45]. Contents of MDA, a peroxidant of membranous phospholipid, can denote the damage degree of membrane. Indeed, our results revealed that over-SUMOylation of PPARγ, like hyperglycemia, significantly elevated the contents of MDA whereas decreased the activities of GSH-Px and SOD−Mn, demonstrating that over-SUMOylation of PPARγ induces the vascular oxidative stress.

Numerous studies indicate ROS can also result in inflammation and IR is also a chronic inflammation [46]. During the inflammation, IKK, an upstream kinase of inhibitory κB α (IκBα), plays critical roles. IKK phosphorylates IκBα at serine 32 and 36, respectively, and phosphorylated IκBα is degraded. Therefore, the hetero-trimer of IκBα-P65-P50 is converted to the hetero-dimer of P65-P50, followed by translocation of P65-P50 from cytoplasm to nucleus where it launches the transcription of target genes encoding inflammatory cytokines including interleukins, interferons, tumor necrotic factors, cellular adhesion molecules and iNOS so on [47]. Our present results showed that over-SUMOylation of PPARγ, like HFD, notably increased the expression levels of IKK-pS176 in aorta, suggesting over-SUMOylation of PPARγ results in IKK activation. Our recent study also shows that activation of IKK and subsequent interaction of IKK and PIAS1 are ROS-dependent. When vitamin E, an antioxidant, was used, activation of IKK and subsequent interaction of IKK and PIAS1 were partially abolished [10].

Finally, we wondered what would happen after IKK activation induced by over-SUMOylation of PPARγ. Besides the canonical NFκB pathway, it has recently been found that IKK also interacts with IRS1 and phosphorylates it at serine 312, resulting in a decrease in the capacity of IRS1 to bind to insulin receptors and thus weakening insulin signal transduction. In our experiment, indeed, we examined the expression levels of PI3K, AKT and eNOS markedly decreased in Ad group, indicating that over-SUMOylation of PPARγ down-regulates the insulin signaling mediated by IKK. PIAS1 is extensively involved in protein SUMOylation. The protein SUMOylation process is a cascade process mediated by Uba2-Ubc9-PIAS1, similar to ubiquitinylation of proteins [48]. PIAS family includes PIAS1, PIAS3, PIASxα and PIASxβ. Among these PIAS, PIAS1 is a rate-limiting enzyme and plays the most important roles in protein SUMOylation [49]. It is thought that PIAS1 highly expresses in vascular endothelial cells [50]. In our experiment, we unexpectedly found an intriguing phenomenon that IKK cross-talked with PIAS1 both HFD and Ad group, suggesting that HFD could induce SUMOylation of PPARγ and the SUMOylation of PPARγ further triggers endogenous SUMOylation process and eventually exacerbates the endothelial IR.

Of course, there were some limitations in this study. For examples, in probe of the effects of PPARγ over-SUMOylation on oxidative stress, we detected only the MDA contents and the activities of GAH-Px and SOD−Mn, but failed to directly measure the ROS levels in vascular tissue; besides, we investigated only the independent effects of HFD and PPARγ over-SUMOylation, it is not clear whether HFD and PPARγ over-SUMOylation have a synergistic effect; moreover, it is not completely identified how SUMOylation of PPARγ results in the repression of insulin signal pathway. While the negatively regulatory effect of SUMOylation of PPARγ on eNOS-NO pathway is independent on TZDs and TZDs benefit for vasculopathy of T2DM, TZDs manifest many cardiovascular side effects. To overcome the shortcomings of TZDs, further studies are needed in the future. In methodology, there are also some shortcomings. For an instance, the approach of forced co-expression of PPARγ, SUMO1 and PIAS1 taken in this study would result in the off-target effect of PPARγ SUMOylation and the non-specific effect on vasculature. A putative better approach to prevent the off-target effects is to construct such an endothelium-specific vector expressing the fusion protein of PPARγ and SUMO1 and such an approach would be utilized in the future study. Despite these limitations, the findings will deepen the understanding on PPARγ SUMOylation-regulating insulin signaling network and offer a potential target for prevention and cure of diabetic vascular complications.

5. Conclusion

In summary, our present study showed that over-SUMOylation of PPARγ, like HFD, induced the endothelial IR and dysfunction in rats. Moreover, we further demonstrated that over-SUMOylation of PPARγ exerts such effects via a down- regulation of PI3K-AKT-eNOS pathway. Besides, we amazingly found that over-SUMOylation of PPARγ triggered the endogenous SUMOylation process and eventually exacerbated the endothelial IR. The findings will deepen the understanding on PPARγ SUMOylation-regulating insulin signaling network and uncover the patho-physiological significance of SUMOylation of PPARγ in diabetic angiopathy. Furthermore, it will offer a potential target for prevention and cure of diabetic vascular complications.

Declaration of Competing Interests

The authors declare no conflict of interests.

Acknowledgement

This study was supported by the grants from the National Natural Scientific Foundation of China (81960153, 81360060, 81070633, and 31660323).

Appendix A. Supplementary data

Supplementary data to this article can be found online at https://doi.org/10.1016/j.vph.2019.106597.

References

[1] C.K. Tan, Y. Zhuang, W. Wahli, Synthetic and natural peroxisome proliferator-activated receptor (PPAR) agonists as candidates for the therapy of the metabolic syndrome, Expert Opin. Ther. Targets 21 (2017) 333–348, https://doi.org/10.1080/14728222.2017.1280467.

[2] A.C. Puhl, F.A. Milton, A. Cvoro, D.H. Sieglaff, J.C. Campos, A. Bernardes, C.S. Filgueira, J.L. Lindemann, T. Deng, F.A. Neves, I. Polikarpov, P. Webb, Mechanisms of peroxisome proliferator activated receptor γ regulation by non-steroidal anti-inflammatory drugs, Nucl. Recept. Signal. 13 (2015) e004, , https://doi.org/10.1621/nrs.13004. eCollection 2015.

[3] S. Sauer, Ligands for the nuclear peroxisome proliferator-activated receptor gamma, Trends Pharmacol. Sci. 36 (2015) 688–704, https://doi.org/10.1016/j.tips.2015.06.010.

[4] K.M. Wadosky, M.S. Willis, The story so far: post-translational regulation of peroxisome proliferator-activated receptors by ubiquitination and SUMOylation, Am. J. Physiol. Heart Circ. Physiol. 302 (2012) H515–H526, https://doi.org/10.1152/ajpheart. 00703. 2011.

[5] R. Brunmeir, F. Xu, Functional regulation of PPARs through post-translational modifications, Int. J. Mol. Sci. 19 (2018), https://doi.org/10.3390/ijms19061738 pii: E1738.

[6] L.A. Stechschulte, P.J. Czernik, Z.C. Rotter, F.N. Tausif, C.A. Corzo, D.P. Marciano, A. Asteian, J. Zheng, J.B. Bruning, T.M. Kamenecka, C.J. Rosen, P.R. Griffin, B. Lecka-Czernik, PPARG post-translational modifications regulate bone formation and bone resorption, EBio. Med. 10 (2016) 174–184, https://doi.org/10.1016/j.ebiom.2016. 06. 040.

[7] S.S. Chung, B.Y. Ahn, M. Kim, J.H. Kho, H.S. Jung, K.S. Park, SUMO modification

selectively regulates transcriptional activity of peroxisome- proliferator-activated receptor γ in C2C12 myotubes, Biochem. J. 433 (2011) 155–161, https://doi.org/10.1042/BJ20100749.
[8] M. Armoni, C. Harel, E. Karnieli, PPARγ gene expression is autoregulated in primary adipocytes: ligand, sumoylation, and isoform specificity, Horm. Metab. Res. 47 (2015) 89–96, https://doi.org/10.1055/s-0034-1394463.
[9] C. Jennewein, A.M. Kuhn, M.V. Schmidt, V. Meilladec-Jullig, A. von Knethen, F.J. Gonzalez, B. Brüne, Sumoylation of peroxisome proliferator-activated receptor gamma by apoptotic cells prevents lipopolysaccharide-induced NCoR removal from kappaB binding sites mediating transrepression of proinflammatory cytokines, J. Immunol. 181 (2008) 5646–5652.
[10] D. Lan, X. Shen, W. Yuan, Y. Zhou, Q. Huang, Sumoylation of PPARγ contributes to vascular endothelium insulin resistance through stabilizing the PPARγ-NcoR complex, J. Cell. Physiol. 234 (2019) 19663–19674, https://doi.org/10.1002/jcp.28567.
[11] H. Li, X. Zhu, A. Wang, G. Wang, Y. Zhang, Co-effect of insulin resistance and biomarkers of inflammation and endothelial dysfunction on hypertension, Hypertens. Res. 35 (2012) 513–517, https://doi.org/10.1038/hr.2011.229.
[12] A. Janus, E. Szahidewicz-Krupska, G. Mazur, A. Doroszko, Insulin resistance and endothelial dysfunction constitute a common therapeutic target in cardiometabolic disorders, Mediat. Inflamm. 2016 (2016) 3634948, , https://doi.org/10.1155/2016/3634948.
[13] A. Rao, V. Pandya, A. Whaley-Connell, Obesity and insulin resistance in resistant hypertension: implications for the kidney, Adv. Chronic Kidney Dis. 22 (2015) 211–217, https://doi.org/10.1053/j.ackd.2014.12.004.
[14] N. Katakami, Mechanism of development of atherosclerosis and cardiovascular disease in diabetes mellitus, J. Atheroscler. Thromb. 25 (2018) 27–39, https://doi.org/10.5551/jat. RV17014.
[15] A. Razuvaev, K. Lund, J. Roy, U. Hedin, K. Caidahl, Noninvasive real-time imaging of intima thickness after rat carotid artery balloon injury using ultrasound biomicroscopy, Atherosclerosis 99 (2008) 310–316.
[16] Z. Meng, J. Li, Q. Zhang, W. Bai, Z. Yang, Y. Zhao, F. Wang, Vasodilator effect of gaseous sulfur dioxide and regulation of its level by Ach in rat vascular tissues, Inhal. Toxicol. 21 (2009) 1223–1228.
[17] C. Ragginer, C. Bernecker, H. Ainoedhofer, S. Pailer, P. Kieslinger, M. Truschnig-Wilders, H.-J. Gruber, Treatment with the nitric oxide donor SNP increases triiodothyronine levels in hyper- and hypothyroid Sprague-Dawley rats, Horm. Metab. Res. 46 (2013) 808–812.
[18] F. Artunc, E. Schleicher, C. Weigert, A. Fritsche, N. Stefan, H.U. Häring, The impact of insulin resistance on the kidney and vasculature, Nat. Rev. Nephrol. 12 (2016) 721–737, https://doi.org/10.1038/nrneph.2016.145.
[19] J.A. Kim, M. Montagnani, K.K. Koh, M.J. Quon, Reciprocal relationships between insulin resistance and endothelial dysfunction: molecular and patho- physiological mechanisms, Circulation 113 (2006) 1888–1904.
[20] M.S. Zhou, I.H. Schulman, L. Raij, Vascular inflammation, insulin resistance, and endothelial dysfunction in salt-sensitive hypertension: role of nuclear factor kappa B activation, J. Hypertens. 28 (2010) 527–535, https://doi.org/10.1097/HJH.0b013e3283340 da8.
[21] C. Manrique, G. Lastra, J.R. Sowers, New insights into insulin action and resistance in the vasculature, Ann. N. Y. Acad. Sci. 1311 (2014) 138–150, https://doi.org/10.1111/nyas.12395.
[22] A.J. Wirix, P.J. Kaspers, J. Nauta, M.J. Chinapaw, J.E. Kist-van Holthe, Pathophysiology of hypertension in obese children: a systematic review, Obes. Rev. 16 (2015) 831–842, https://doi.org/10.1111/obr.12305.
[23] S. Cook, O. Hugli, M. Egli, B. Ménard, S. Thalmann, C. Sartori, C. Perrin, P. Nicod, B. Thorens, P. Vollenweider, U. Scherrer, R. Burcelin, Partial gene deletion of endothelial nitric oxide synthase predisposes to exaggerated high-fat diet- induced insulin resistance and arterial hypertension, Diabetes 53 (2004) 2067–2072.
[24] S.J. Cleland, J.R. Petrie, M. Small, H.L. Elliott, J.M. Connell, Insulin action is associated with endothelial function in hypertension and type 2 diabetes, Hypertension 35 (2000) 507–511.
[25] L.X. Cubeddu, I.S. Hoffmann, Insulin resistance and upper-normal glucose levels in hypertension: a review, J. Hum. Hypertens. 16 (2002) S52–S55.
[26] S. Sitia, L. Tomasoni, F. Atzeni, G. Ambrosio, C. Cordiano, A. Catapano, S. Tramontana, F. Perticone, P. Naccarato, P. Camici, E. Picano, L. Cortigiani, M. Bevilacqua, L. Milazzo, D. Cusi, C. Barlassina, P. Sarzi-Puttini, M. Turiel, From endothelial dysfunction to atherosclerosis, Autoimmun. Rev. 9 (2010) 830–834, https://doi.org/10.1016/j.autrev. 2010. 07.016.
[27] S.H. Ihm, S.W. Jang, O.R. Kim, K. Chang, M.H. Oak, J.O. Lee, D.Y. Lim, J.H. Kim, Decaffeinated green tea extract improves hypertension and insulin resistance in a rat model of metabolic syndrome, Atherosclerosis 224 (2012) 377–383, https://doi.org/10.1016/j.atherosclerosis.2012.07.006.
[28] M. Toral, M. Gómez-Guzmán, R. Jiménez, M. Romero, M.J. Zarzuelo, M.P. Utrilla, C. Hermenegildo, Á. Cogolludo, F. Pérez-Vizcaíno, J. Gálvez, J. Duarte, Chronic peroxisome proliferator-activated receptorβ/δ agonist GW0742 prevents hypertension, vascular inflammatory and oxidative status, and endothelial dysfunction in diet-induced obesity, J. Hypertens. 33 (2015) 1831–1844, https://doi.org/10.1097/HJH.00000 00000000634.
[29] H. Duplain, R. Burcelin, C. Sartori, S. Cook, M. Egli, M. Lepori, P. Vollenweider, T. Pedrazzini, P. Nicod, B. Thorens, U. Scherrer, Insulin resistance, hyperlipidemia, and hypertension in mice lacking endothelial nitric oxide synthase, Circulation 104 (2001) 342–345.
[30] R.T. de Jongh, E.H. Serné, R.G. Ijzerman, C.D. Stehouwer, Microvascular function: a potential link between salt sensitivity, insulin resistance and hypertension, J. Hypertens. 25 (2007) 1887–1893.
[31] B. Gross, M. Pawlak, P. Lefebvre, B. Staels, PPARs in obesity-induced T2DM, dyslipidaemia and NAFLD, Nat. Rev. Endocrinol. 13 (2017) 36–49, https://doi.org/10.1038/nrendo.2016.135.
[32] C. Maccallini, A. Mollica, R. Amoroso, The positive regulation of eNOS signaling by PPAR agonists in cardiovascular diseases, Am. J. Cardiovasc. Drugs 17 (2017) 273–281, https://doi.org/10.1007/s40256-017-0220-9.
[33] F.A. Monsalve, R.D. Pyarasani, F. Delgado-Lopez, R. Moore-Carrasco, Peroxisome proliferator-activated receptor targets for the treatment of metabolic diseases, Mediat. Inflamm. 2013 (2013) 549627, , https://doi.org/10.1155/2013/549627.
[34] S.E. Inzucchi, C.M. Viscoli, L.H. Young, K.L. Furie, M. Gorman, A.M. Lovejoy, S. Dagogo-Jack, F. Ismail-Beigi, M.T. Korytkowski, R.E. Pratley, G.G. Schwartz, W.N. Kernan, IRIS trial investigators, pioglitazone prevents diabetes in patients with insulin resistance and cerebrovascular disease, Diabetes Care 39 (2016) 1684–1692, https://doi.org/10.2337/dc16-0798.
[35] T. Katafuchi, W.L. Holland, R.K. Kollipara, R. Kittler, D.J. Mangelsdorf, S.A. Kliewer, PPARγ-K107 SUMOylation regulates insulin sensitivity but not adiposity in mice, Proc. Natl. Acad. Sci. U. S. A. 115 (2018) 12102–12111, https://doi.org/10.1073/pnas.18145 22115.
[36] T. Ohshima, H. Koga, K. Shimotohno, Transcriptional activity of peroxisome proliferator-activated receptor gamma is modulated by SUMO-1 modification, J. Biol. Chem. 279 (2004) 29551–29557.
[37] P.A. Dutchak, T. Katafuchi, A.L. Bookout, J.H. Choi, R.T. Yu, D.J. Mangelsdorf, S.A. Kliewer, Fibroblast growth factor-21 regulates PPARγ activity and the antidiabetic actions of thiazolidinediones, Cell 148 (2012) 556–567.
[38] J.A. García, F. Ortiz, J. Miana, C. Doerrier, M. Fernández-Ortiz, I. Rusanova, G. Escames, J.J. García, D. Acuña-Castroviejo, Contribution of inducible and neuronal nitric oxide synthases to mitochondrial damage and melatonin rescue in LPS-treated mice, J. Physiol. Biochem. 73 (2017) 235–244, https://doi.org/10.1007/s13105-017 -0548-2.
[39] P. Kosutova, P. Mikolka, M. Kolomaznik, S. Balentova, A. Calkovska, D. Mokra, Effects of S-nitroso-N-acetyl-penicillamine (SNAP) on inflammation, lung tissue apoptosis and iNOS activity in a rabbit model of acute lung injury, Adv. Exp. Med. Biol. 935 (2016) 13–23, https://doi.org/10.1007/5584-2016-34.
[40] A.V. Araújo, C.Z. Ferezin, C. Pereira Ade, G.J. Rodrigues, M.D. Grando, D. Bonaventura, L.M. Bendhack, Augmented nitric oxide production and up-regulation of endothelial nitric oxide synthase during cecal ligation and perforation, Nitric Oxide 27 (2012) 59–66, https://doi.org/10.1016/j.niox.2012.04.005.
[41] N. Fujimura, D. Jitsuiki, T. Maruhashi, S. Mikami, Y. Iwamoto, M. Kajikawa, K. Chayama, Y. Kihara, K. Noma, C. Goto, Y. Higashi, Geranylgeranylacetone, heat shock protein 90/AMP-activated protein kinase/endothelial nitric oxide synthase/nitric oxide pathway, and endothelial function in humans, Arterioscler. Thromb. Vasc. Biol. 32 (2012) 153–160, https://doi.org/10.1161/ATVBAHA.111.237263.
[42] J.L. Rains, S.K. Jain, Oxidative stress, insulin signaling, and diabetes, Free Radic. Biol. Med. 50 (2011) 567–575, https://doi.org/10.1016/j.freeradbiomed.2010.12.006.
[43] R.E. Lamb, B.J. Goldstein, Modulating an oxidative-inflammatory cascade: potential new treatment strategy for improving glucose metabolism, insulin resistance, and vascular function, Int. J. Clin. Pract. 62 (2008) 1087–1095, https://doi.org/10.1111/j.1742 -1241. 2008.01789.x.
[44] J.C. Cruz, A.F. Flôr, M.S. França-Silva, C.M. Balarini, V.A. Braga, Reactive oxygen species in the paraventricular nucleus of the hypothalamus alter sympathetic activity during metabolic syndrome, Front. Physiol. 6 (2015) 384, https://doi.org/10.3389/fphys.2015.00384.
[45] P. Wenzel, S. Kossmann, T. Münzel, A. Daiber, Redox regulation of cardiovascular inflammation-immunomodulatory function of mitochondrial and NOX-derived reactive oxygen and nitrogen species, Free Radic. Biol. Med. 109 (2017) 48–60, https://doi.org/10.1016/j.freeradbiomed.2017.01.027.
[46] H. Blaser, C. Dostert, T.W. Mak, D. Brenner, TNF and ROS crosstalk in inflammation, Trends Cell Biol. 26 (2016) 249–261, https://doi.org/10.1016/j.tcb. 2015. 12.002.
[47] C.H. Ma, C.H. Wu, I.M. Jou, Y.K. Tu, C.H. Hung, P.L. Hsieh, K.L. Tsai, PKR activation causes inflammation and MMP-13 secretion in human degenerated articular chondrocytes, Redox Biol. 14 (2018) 72–81, https://doi.org/10.1016/j.redox.2017.08.011.
[48] A. Flotho, F. Melchior, Sumoylation: a regulatory protein modification in health and disease, Annu. Rev. Biochem. 82 (2013) 357–385, https://doi.org/10.1146/annurev-biochem- 061909-093311.
[49] R. Rott, R. Szargel, V. Shani, H. Hamza, M. Savyon, F. Abd Elghani, R. Bandopadhyay, S. Engelender, SUMOylation and ubiquitination reciprocally regulate α-synuclein degradation and pathological aggregation, Proc. Natl. Acad. Sci. U. S. A. 114 (2017) 13176–13181, https://doi.org/10.1073/pnas.1704351114.
[50] K.S. Heo, E. Chang, Y. Takei, N.T. Le, C.H. Woo, M.A. Sullivan, C. Morrell, K. Fujiwara, J. Abe, Phosphorylation of protein inhibitor of activated STAT1 (PIAS1) by MAPK-activated proteinkinase-2 inhibits endothelial inflammation via increasing both PIAS1 transrepression and SUMO E3 ligase activity, Arterioscler. Thromb. Vasc. Biol. 33 (2013) 321–329, https://doi.org/10.1161/ATVBAHA.112.300619.